Transactions of the Materials Research Society of Japan 31[1] 169-171 (2006)

Electrode Dependence of Thermally Stimulated Current in PZT Thin Film Capacitors

Takashi Nishida, Yoshinari Nakayama, Takashi Takeda, Kiyoshi Uchiyama and Tadashi Shiosaki

Graduate School of Materials Science, Nara Institute of Science and Technology (NAIST) 8916-5 TAKAYAMA-CHO, IKOMA, NARA 630-0101, JAPAN

Fax: 81-743-72-6069; E-mail: tnishida@ms.naist.jp

PZT film capacitors were fabricated with various thicknesses and different electrode materials by sputter deposition, and their thermally stimulated current (TSC) properties were evaluated. The crystalline defects in the films were investigated. Two trap levels with activation energies of 0.7eV and 0.9eV were observed in the TSC measurements. The 0.9eV trap increased with degradation, such as by fatigue or composition change. The 0.7eV trap was influenced by the top electrode. In the case of an Ir top electrode, the 0.7eV trap vanished. This trap seems to exist in the boundary region between the top electrode and the PZT layer, based on the thickness dependence measurements. The origins and distribution of crystalline defects in PZT films were thus revealed by the TSC properties.

Key words: TSC, PZT, Ir electrode, crystalline defects, trap level

1. INTRODUCTION

$Pb(Zr_xTi_{1-x})O_3$ (PZT) thin films are useful for fabricating a number of electronic devices such as ferroelectric random access memories (FeRAM) and micro-electromechanical systems (MEMS) devices. However, capacitors made from the films show degradation problems such as from fatigue, imprinting, etc. because of crystalline defects in the films, and defect properties and their improvements have therefore been studied widely. [1-3] Degradation mechanisms have been investigated by current measurements and temperature dependence. [4-6] In particular, thermally stimulated current (TSC) measurement may be a useful method for evaluation of defects because information on activation energy and density of trap levels caused by the defects can be determined. Experiments on the dependence of TSC on fatigue properties have been performed, and an increase in trap density by degradation can be observed by TSC measurements. [7,8]

We have previously investigated crystalline defects in PZT films using TSC, and have reported the relationship between TSC and PZT film composition. [9] Two trap levels are observed from the TSC peaks, revealing that one of the trap levels is related to both the degradations and the composition of lead and oxygen. However, information on the other peak as well as the influence of the electrode/PZT interface has not yet been obtained. In this paper, we report on the preparation of PZT thin film capacitors with Pt and Ir electrodes, and we evaluate the dependence of TSC on the electrode material.

2. EXPERIMENTAL

PZT thin films were deposited on Pt/SiO2/Si substrates by rf-magnetron sputtering. The sputtering conditions are summarized in Table I. The films obtained were crystallized by furness annealing at 600°C in air. The composition and crystal orientation of the PZT films were measured by X-ray fluorescence analysis and X-ray diffraction (XRD), respectively, and (111)-oriented PZT films (Zr/Ti=40/60) were used in the experiments. The Pt and Ir top electrodes were also prepared by sputtering, and electrode patterns with 0.13mm diameter were formed by metal mask methods. An annealing treatment of the capacitors at 600°C in air was performed to improve their electrical properties.

The electrical properties of D-E hysteresis and the leakage current of Pt/PZT/Pt and Ir/PZT/Pt capacitors obtained were measured using a ferroelectric capacitor tester (TF-2000FE, aixACCT). TSC measurements for the capacitors were then performed. The measurement procedure was reported in our previous paper in detail. [9] The system was constructed using an electrometer (K6517, Keithley), a temperature controller (FP21, Shimaden) and a heater stage in a vacuum chamber. The measurement conditions are summarized in Table II.

Table I. Sputtering conditions

Temperature	350°C
rf power	
$Pb(Zr_{0.5}Ti_{0.5})O_3$	500W
PbO	50W
TiO_2	300W
Gas Ar:O_2 (SCCM)	9:2
Gas Pressure	1.5Pa
Time	60min

Table II. TSC measurement conditions

Temperature Range	R.T. – 280°C
Heating Rate	2K/min
Trapping Voltage	1.0V
Collection Voltage	5.0mV

3. RESULTS AND DISCUSSION

Figure 1 shows the crystalline and ferroelectric properties of PZT films with 200nm thickness. The (111)-oriented PZT films were obtained on the Pt(111) bottom electrode layer, as shown in Fig. 1(a). Pt and Ir top electrodes were prepared on the PZT layers, and ferroelectric hysteresis curves were observed at both electrodes (Fig. 1(b)). However, larger remnant polarization (*Pr*) was obtained with the Ir electrode ($2Pr$=46μC/cm^2) than the Pt electrode ($2Pr$=63μC/cm^2). Also, the fatigue performance were slightly improved by the Ir top electrode, as shown in Fig. 1 (c).

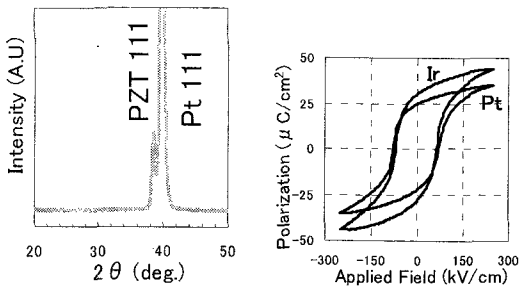

(a) XRD pattern (b) DE hysteresis loop

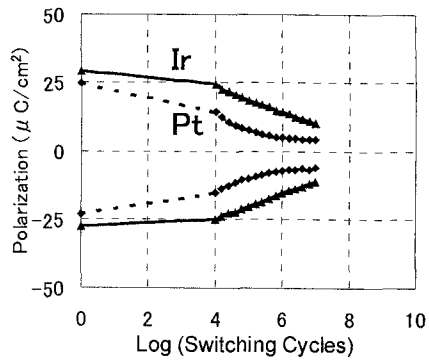

(c) Fatigue

Fig. 1 XRD pattern and ferroelectric properties of the PZT film capacitors.

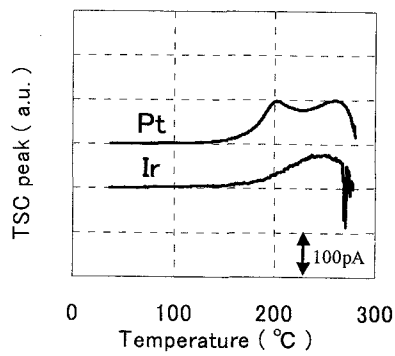

Fig. 2 TSC of PZT (400nm thickness) capacitors with Pt and Ir top electrodes.

TSC of the PZT capacitors was measured, and the obvious TSC peaks are shown in Fig. 2. In the case of the Pt/PZT/Pt structure, two TSC peaks (peak I at 200°C and peak II at 250°C) were obtained. From previous work, peak II increased both by fatigue and by the composition shift of lead and oxygen, revealing that peak II is related to degradation. [9] On the other hand, degradation affected peak I minimally, and the origin of peak I has not been determined. In the case of the Ir top electrode, peak II was also obtained; however, peak I vanished, as shown in Fig. 2, revealing that peak I is related to the trap level at the interface between the top electrode and the PZT layer.

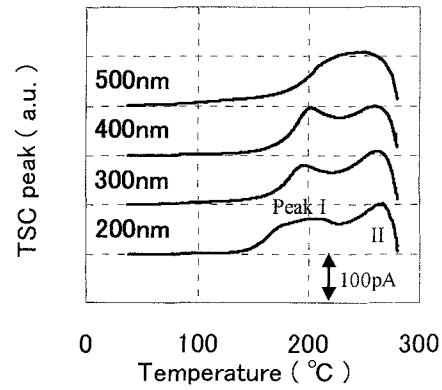

Fig. 3 The thickness dependence of TSC for the Pt/PZT/Pt capacitors.

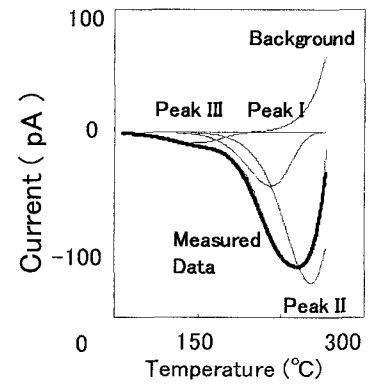

Fig. 4 Curve-fitting analysis of TSC for 500nm-thick PZT.

Figure 3 shows the thickness dependence of TSC. The peak intensities of both peak I and peak II were not affected by the thickness; hence, crystalline defects were located in the interface layer. Peak I decreased for the 500nm-thick sample because the surface condition seems to be different for such a thick film. However, from curve fitting, both peaks were contained in the TSC curve, as shown in Fig. 4. The activation energies of peak I and II are determined to be 0.75eV and 0.85eV, respectively. These values agree with results from the previous report. [9] Trap density can be estimated from the total charge calculated by integrating the TSC, and the charge densities (*Nc*) of peaks I and II were 8.3x10^{19} cm^{-3} and 2.1x10^{20} cm^{-3}, respectively. The trap center density (*Nt*) is higher than *Nc* due to charge recombination. Thus, *Nt* was determined from the mobility μ and the lifetime τ as,

$$Nt = Nc\, d^2 / (\tau\, \mu\, V).$$

Here, *d* is the thickness, and *V* is the applied voltage. Assuming μ=0.1cm^2/Vs [10] and τ=1x10^{-8}s [11], the trap densities obtained for peak I and II were

$4.1x10^{22}cm^{-3}$ and $1.0x10^{23}cm^{-3}$, respectively. These densities are considerably larger than the typical value ($\sim10^{21}cm^{-3}$) [1,8] because the applied voltage and charge were concentrated in a narrow interface layer [12], and effective *d* and Nt may have decreased appreciably.

Another weak peak was also found at a lower temperature of 140°C. The activation energy of this peak was calculated to be 0.39eV. This trap level seems to be located in the whole film since the peak cannot be obtained for thinner films, and trap levels of 0.2-0.4eV related to Pb^{3+} in bulk $PbTiO_3$ ceramics were reported. [13,14]

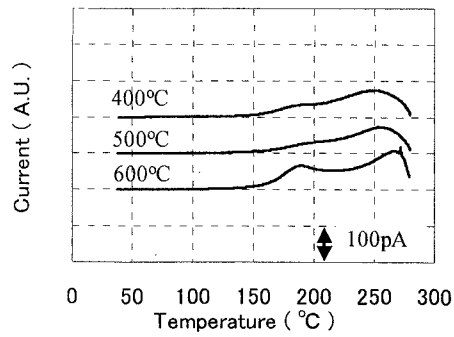

Fig. 5 The dependence of TSC on the temperature of recovery annealing.

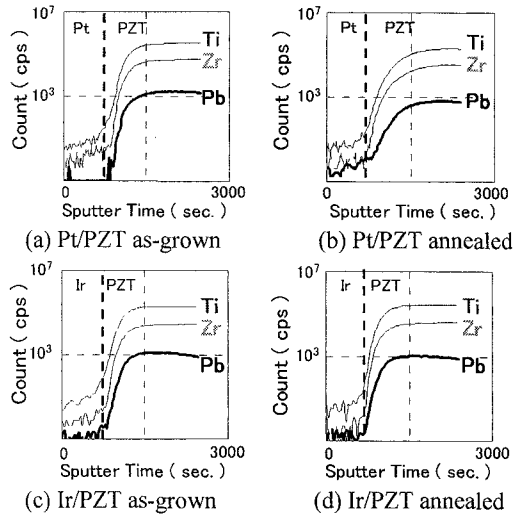

Fig. 6 SIMS depth profiles of the PZT thin film capacitors.

The dependence of TSC on annealing temperature after the top electrode deposition was also evaluated, as shown in Fig. 5. The intensity of peak I decreased with decreasing annealing temperature. Since inter-diffusion between the top Pt layer and the PZT layer occurred at a high temperature, a defect layer at the interface (peak I) was formed. Figure 6 shows the SIMS depth profiles of the PZT capacitors. The diffusion of Pb to the electrode layer by annealing was observed only in the capacitor with the Pt top electrode, as shown in Fig. 6 (b). This is suggests that inter-diffusion occurred at the Pt/PZT interface, and crystalline defects were formed by annealing.

4. CONCLUSIONS

The electrode material dependence of TSC in PZT film capacitors was evaluated. The TSC peak (peak I) at a lower temperature (200°C) was affected by the electrode material and annealing temperature after deposition of top electrodes; however, the peaks were not obviously affected by the thickness of the PZT layer. The trap center density estimated was high ($\sim10^{22}cm^{-3}$). From these results, it is revealed that peak I is related to the crystalline defects located in the interface between the top electrode and the PZT layer, and the defects increased by inter-diffusion at this interface during the annealing treatment. Further, SIMS depth profile evaluation of the films revealed the diffusion of lead.

ACKNOWLEDGEMENTS

The authors would like to thank Mr. Yasuo Okajima for SIMS measurements, Mr. Claus Schroeter for providing the Linux-GPIB package, and Dr. Toshihisa Horiuchi for consultations on the fabrication of the TSC system. We are also grateful to Dr. Yoichiro Masuda for his encouragement during this study. This work was partly supported by the Murata Science Foundation and a Grant-in-Aid for Scientific Research (12750273) by the Japan Society for the Promotion of Science.

REFERENCES

[1] T. Mihara, H. Watanabe and C.A. Araujo, Jpn. J. Appl. Phys., 33, 3996-4002 (1994).
[2] T. Nakamura, Y. Nakao, A. Kamisawa and H. Takasu, Jpn. J. Appl. Phys., 33, 5207-5210 (1994).
[3] T. Nishida, I. Kawakami, M. Norimoto and T. Shiosaki, Ceramics International, 30, 1089-1093 (2004).
[4] J.F. Scott, B.M. Melnick, J.D. Cuchiaro, R. Zuleeg, C.A. Araujo, L.D. McMillan and M.C. Scott, Integ. Ferro., 4, 85-92 (1994).
[5] T. Mihara, H. Watanabe and C.A. Araujo, Jpn. J. Appl. Phys., 33, 5281-5286 (1994).
[6] Y. Masuda and T. Nozaka, Jpn. J. Appl. Phys., 43, 6576-6580 (2004).
[7] H. Okino, Y. Toyoda, M. Shimizu, T. Horiuchi, T. Shiosaki and K. Matsushige, Jpn. J. Appl. Phys., 37, 5137-5140 (1994).
[8] Z. Wu and M. Sayer, Proc. ISAF (IEEE, New York) 244-247 (1994).
[9] T. Nishida, M. Matsuoka, S. Okamura and T. Shiosaki, Jpn. J. Appl. Phys., 42, 5947-5951 (2003).
[10] G.M. Choi, H.L. Tuller and D. Goldschmidt, Phys Rev B34, 6972 (1986).
[11] S. Thakoor, A. P. Thakoor, and S. E. Bernacki, Proc Int. Symp. Integ. Ferro., 3, 262 (1991).
[12] J. F. Scott, "Ferroelectric Memories" Springer Verlag (2000) pp. 95-96
[13] L. Pintile, M. Alexe, I. Pintile and I. Boierasu, Ferroelec., 201, 217 (1997).
[14] J. Robertson and W.L. Warren, MRS Proc. 361, 117 (1985).

(Received December 20, 2005; Accepted January 31, 2006)